



Diagnostics of Western Himalayan Satluj River flow: Warm season (MAM/JJAS) inflow into Bhakra dam in India

Indrani Pal^{a,b,*}, Upmanu Lall^c, Andrew W. Robertson^b, Mark A. Cane^d, Rajeev Bansal^e

^a Department of Civil Engineering, University of Colorado Denver, CO 80204, United States

^b International Research Institute for Climate and Society, The Earth Institute at Columbia University, Palisades, NY 10964, United States

^c Department of Earth and Environmental Engineering, Columbia University, New York, NY 10027, United States

^d Lamont-Doherty Earth Observatory, Columbia University, Palisades, NY 10964, United States

^e Bhakra Beas Management Board, Punjab, India

ARTICLE INFO

Article history:

Received 17 May 2012

Received in revised form 9 October 2012

Accepted 22 November 2012

Available online 3 December 2012

This manuscript was handled by

Konstantine P. Georgakakos, Editor-in-Chief,

with the assistance of Matthew Rodell,

Associate Editor

Keywords:

MAM

JJAS inflow

Bhakra dam

Satluj River

Western Himalaya

Diagnostics

SUMMARY

Here we analyze the variability of MAM (March–April–May) and JJAS (June–July–August–September) seasonal Satluj River flow into the Bhakra dam in India through Pearson anomaly correlation and composite analyses with antecedent and concurrent seasonal climatic and atmospheric circulation patterns. The MAM seasonal inflow of Bhakra dam is significantly correlated with winter (DJF/FM) precipitation and temperature of the Satluj basin while the correlation with FM was more prominent for precipitation (snow = +0.72, rainfall = +0.60), and temperature (diurnal temperature range (DTR) = −0.76 and maximum temperature (T_{max}) = −0.57). The JJAS inflow was also positively correlated with DJF/FM as well as JJAS precipitation of the Satluj basin while the correlation with basin average FM was the largest (+0.54). These suggested that both MAM and JJAS inflow anomalies are linked with DJF/FM climate over the Western Himalayas and adjoining north and central Indian plains, which were also found to be linked with the fluctuation of equatorial concurrent Sea Surface Temperature anomalies over the western Indian Ocean (max anomaly correlation was > +0.70) and mean sea level pressure over western pole of the Southern Oscillation sea-saw region (max Pearson anomaly correlation was ~ +0.60). Low (high) MAM inflow was found to be associated with negative (positive) precipitation anomalies over the basin and north India in DJF and FM while FM precipitation anomaly is more concentrated over the Western Himalayas. In addition, low (high) JJAS inflow is also associated with negative (positive) precipitation anomalies over the basin and north India in DJF and over the Western Himalaya in FM and JJAS. Negative geopotential height anomaly at 500 h Pa (Z500) over Siberia and northwestern Pacific in DJF, and positive Z500 anomaly over the northwest India in FM were noticed in low MAM inflow years. Whereas high inflow in MAM was linked with a negative Z500 anomaly between two positive Z500 anomaly regions – one over eastern Siberia stretched up to northern Pacific and second over the Eastern Europe in DJF, which gets stronger in FM. We also found southwesterly (northeasterly) wind vectors at 850 h Pa pressure level (uv850) bringing more (less) moisture to the Western Himalayas in DJF and FM in high (low) MAM/JJAS flow years.

© 2012 Elsevier B.V. All rights reserved.

1. Introduction

The major river systems of the Indian subcontinent that originate in the Himalayas are expected to be very sensitive to climate change because of substantial contributions from the snow and glacier melt (Singh and Jain, 2002). Winter precipitation in the form of snow over the Western Himalayas feed the glaciers, which serve as a vast storehouse of freshwater for the Indus river basin, which provides the primary water supply for the breadbaskets of

* Corresponding author. Address: Department of Civil Engineering, University of Colorado Denver, CO 80204, United States. Tel.: +1 303 352 3804.

E-mail address: indrani.pal@ucdenver.edu (I. Pal).

India and Punjab. The supply of water through these rivers is important for ecological habitats, power generation and irrigation in the following seasons.

The Bhakra dam across Satluj River in north India is the major point of water supply (irrigation to 10 million acres of land) and electricity generation (1325 MW) for the neighboring states of Punjab, Rajasthan and Haryana, including the national capital territory of Delhi. The irrigation canal systems connected with Satluj River and Bhakra dam in India turned the Punjab into the breadbasket of the country, providing the agrarian economic foundation for the arid provinces and feeding the majority of the populations approximately since early 1960s. Bhakra inflow is a joint contribution of the flow from Satluj River and Beas Satluj Link channel,

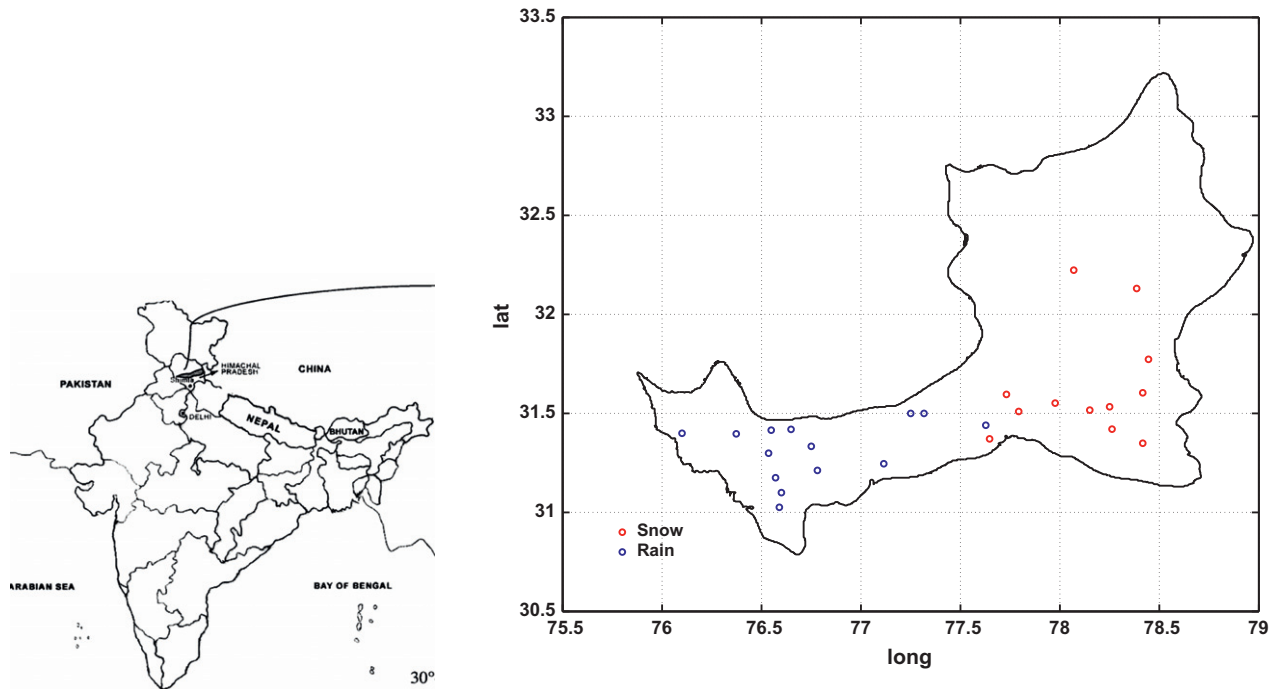


Fig. 1. Indian part of Satluj River basin up to Bhakra reservoir with location of hydro-meteorological stations.

which came into effect in 1977. Thus, cold season precipitation in the Western Himalayas in the form of snow has the major contribution to the total volume of MAM inflow of Bhakra. That also contributes to some extent to JJAS flow in addition to summer monsoon precipitation (Singh and Quick, 1993). Melting snow and ice provides the water supply to much of the north Indian regions under Bhakra command before summer monsoon starts.

Satluj and Beas Rivers originate from the Western Himalayas at different elevations. Through a diversion (Beas Satluj Link/BSL) Beas River is one of the major tributaries of Satluj River. Both are major tributaries of the Indus River; together with another tributary Ravi carrying about 1/5th of annual Indus River flow ($\sim 112 \text{ km}^3$) (Sen Gupta and Desa, 2001). NDJFM (winter) precipitation in the Western Himalayas is mainly associated with the mid-latitude jet stream and low-pressure synoptic systems known as Western Disturbances (WD) (Dimri, 2005, 2006; Yadav et al., 2009). WDs originate over the Mediterranean Sea or North Atlantic Ocean, with secondaries developing over the Persian Gulf and Caspian Sea either directly or as a result of the arrival of low-pressure systems from southwest Arabia, and travel eastward over southwest central Asia (including countries such as Iraq, Iran, Afghanistan, Turkmenistan, Uzbekistan, Kazakhstan, as well as parts of eastern Europe), Pakistan, and northwest India (Mariotti, 2007; Dimri, 2007). In the NDJFM months the midlatitude depressions move to their lowest latitudes and in their pathway travel across the north and central parts of India in a phased manner from west to east, disturbing the normal circulation patterns (Yadav et al., 2009, 2010). Past theoretical and synoptic studies indicated that the development of WDs in the mid-latitudinal synoptic system is associated with baroclinic activity and therefore potential energy residing in the latitudinal temperature gradient is the main source of energy (Rao and Rao, 1971; Dimri et al., 2004).

Past diagnostic studies have focused on DJF circulation patterns during the years of extreme precipitation events (deficit and surplus) over Western Himalayas considering the region of 15°S –

Table 1

Information about different meteorological stations in Satluj River basin in India.

Station name	Latitude (N)	Longitude (E)	Elevation (mAMSL)
<i>Rainfall</i>			
Berthin	31°25'11"	76°38'55"	668
Bhartgarh	31°6'0"	76°36'0"	284
Daslehra	31°24'56"	76°32'56"	562
Ganguwal	31°24'	76°6'	1220
Ghanauli	31°1'33"	76°35'22"	293
Kahu	31°12'43"	76°46'52"	526
Lohand	31°10'31"	76°34'14"	288
Naina Devi	31°17'56"	76°32'8"	985
Nangal	31°23'50"	76°22'21"	369
Rampur	31°26'24"	77°37'40"	987
Suni	31°14'43"	77°6'53"	701
Kasol	31°30'0"	77°19'0"	2614
Kotla	31°30'0"	77°15'0"	2824
Swarghat	31°20'	76°45'	1220
<i>Snow measurement</i>			
Bahli	31°22'17"	77°38'48"	2285
Chitkul	31°20'59"	78°25'0"	3327
Giabong	31°46'24"	78°26'44"	2926
Jangi	31°36'15"	78°25'0"	2721
Kalpa	31°31'60"	78°15'0"	2662
Kaza	32°13'25"	78°4'11"	3618
Kilba	31°31'0"	78°9'0"	1988
Nichar	31°33'7"	77°58'34"	2225
Phancha	31°35'45"	77°43'54"	2348
Sangla	31°25'14"	78°15'44"	2780
Sarhan	31°30'34"	77°47'34"	2144
Tabo	32°7'51"	78°23'11"	4201
<i>Maximum temperature</i>			
Bhakra ^a	31°24'56"	76°26'5"	554
Kasol	31°30'0"	77°19'0"	2614
Nangal ^a	31°23'50"	76°22'21"	369
Rampur	31°26'24"	77°37'40"	987
Suni	31°14'43"	77°6'53"	701

^a Also minimum temperature stations.

45°N and 30°E – 120°E (Dimri et al., 2004; Dimri, 2005, 2006; Yadav et al., 2009, 2010). The large-scale land–ocean interaction and teleconnections and especially the effects of Indian Ocean or

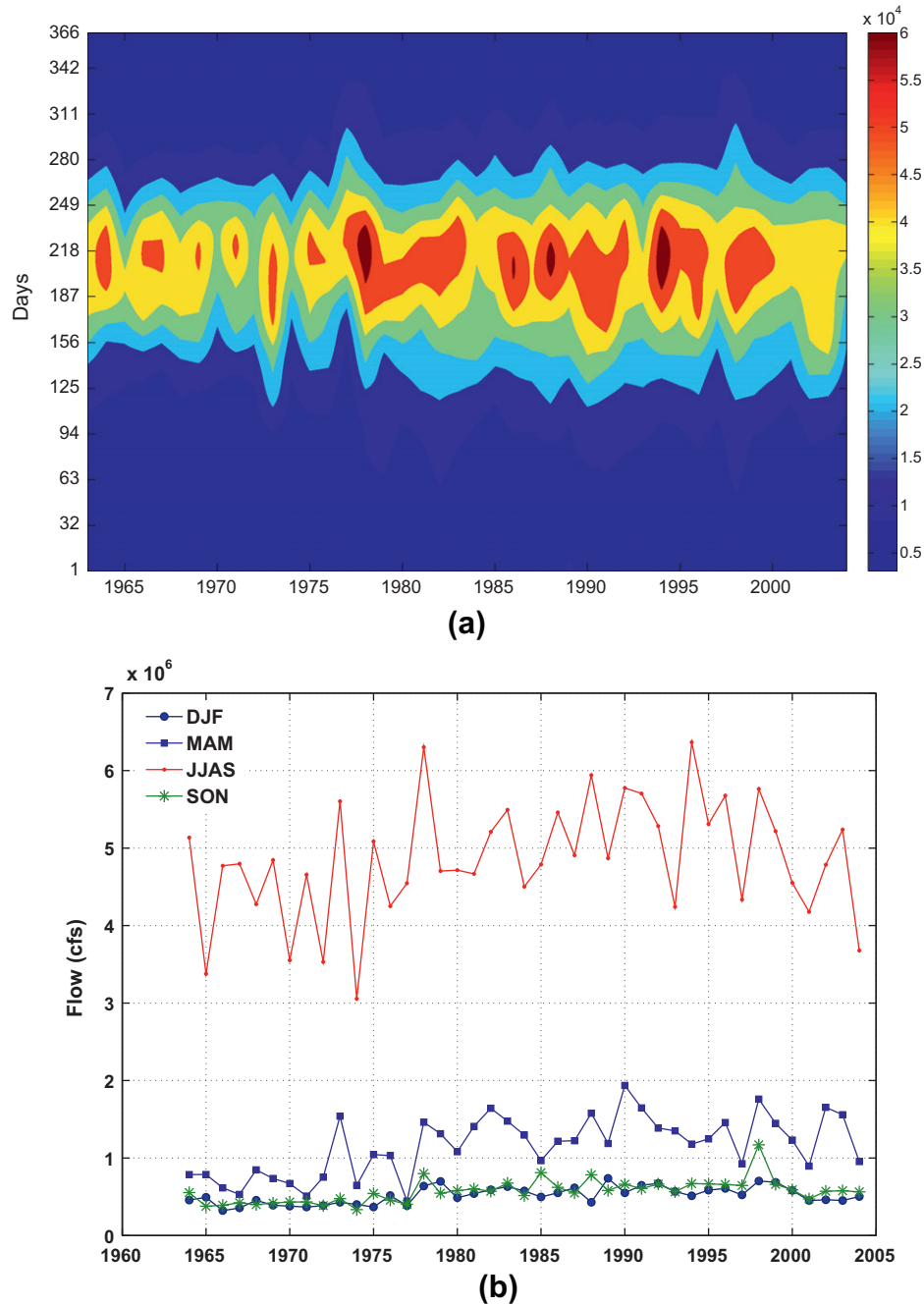


Fig. 2. (a) Contour map of daily inflow (z axis in cfs) and (b) seasonal total inflow to Bhakra reservoir across Satluj River in northern India.

Pacific SST and pressure fields in modulating the concurrent air circulation patterns that ultimately affects the Himalayan local hydrology, have not been well studied. Since WDs occur in NDJFM months and deposit snow in the Western Himalayas, FM/late winter precipitation modulate MAM/JJAS river flow while summer monsoon seasonal precipitation also sustains a large portion of JJAS flow as well (Singh and Quick, 1993). Barlow and Tippet (2008) found that warm season (AMJJA) river flows in central Asia is closely related to regional-scale climate variability of the preceding cold season (NDJFM). Therefore, we want to explore the variability of MAM and JJAS inflow of Bhakra dam linked with large-scale atmospheric circulation patterns and related climate precursors in DJF, FM and JJAS, which primarily affect the interannual variability of volume of precipitation over the Western Himalayas.

2. Study area, data and climatology

The Indian part of Satluj River basin upstream of Bhakra dam is the prime area of interest here. The location of the basin in India is shown in Fig. 1 that also shows the hydro-meteorological station locations. The stations, which were used for the snow measurement data are shown in red¹ and the rainfall measurement stations are shown in blue. Satluj River is a major tributary of the Indus River. Its source is the Rakas lake in Tibet on the southern slopes of Mount Kailash and it flows generally west and southwest entering India

¹ For interpretation of color in Figs. 1 and 7, the reader is referred to the web version of this article.

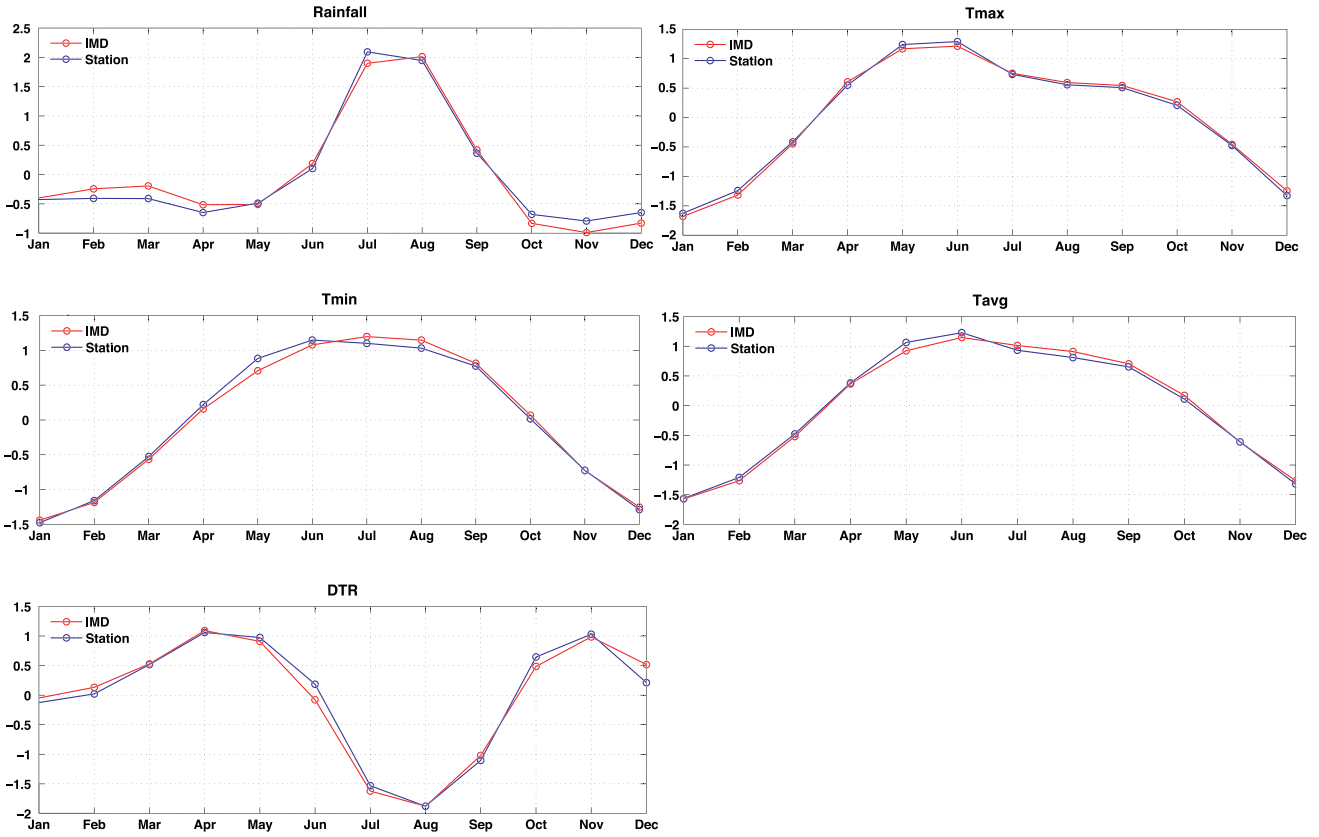


Fig. 3. Comparison of station and IMD local climatology (T_{max} = Normalized maximum temperature; T_{min} = Normalized minimum temperature; T_{avg} = Normalized average temperature; DTR = Normalized diurnal temperature range).

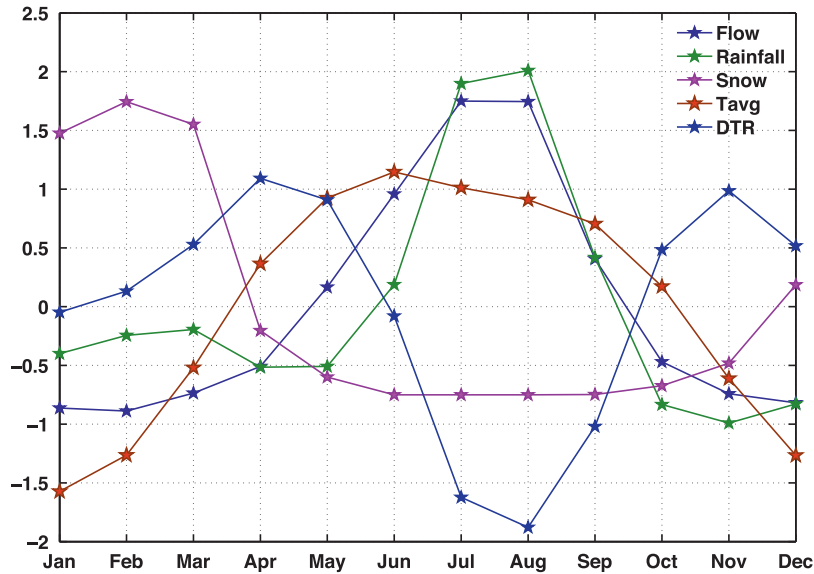


Fig. 4. Normalized (w.r.t. standard deviation after removing mean) monthly inflow and local climatology (T_{avg} = Normalized average temperature; DTR = Diurnal temperature range).

through the Shipki La pass in Himachal Pradesh. It leaves Himachal Pradesh to enter the plains of Punjab at Bhakra, where the world's highest gravity dam has been constructed on this river in 1963. The Satluj finally drains into the Indus in Pakistan. The upper territories of the Satluj River catchment area of about 50,140 km² are located above the permanent snowline. The Beas River is the second easternmost of the rivers of the Punjab, a tributary of Satluj. The riv-

er rises at Rohtang Pass of central Himachal Pradesh, India, and flows for some 470 km to the Satluj River in the Punjab state of India.

The Satluj River basin experiences two flow seasons, MAM (spring) and JJAS (monsoon), which contribute to 18% and 66% of total annual flow respectively. MAM flow primarily comes from the runoff generated by snowmelt from the Western Himalayas while local orographic precipitation events also contribute to the

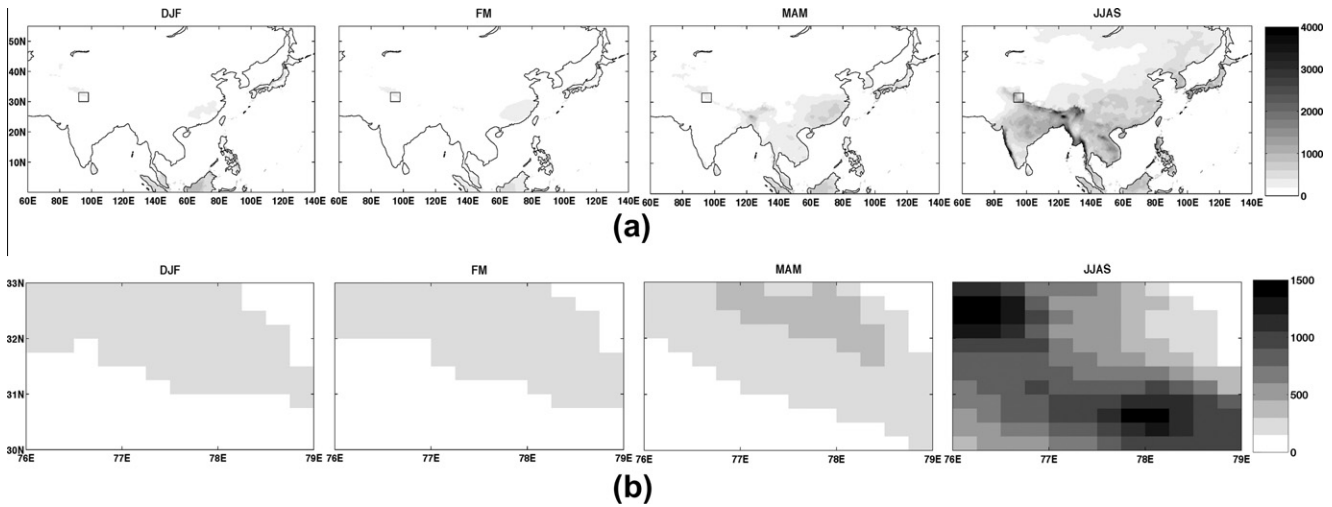


Fig. 5. Climatology of seasonal precipitation total (mm/season) (a) Monsoon Asia and (b) Satluj basin region (data: APHRODITE).

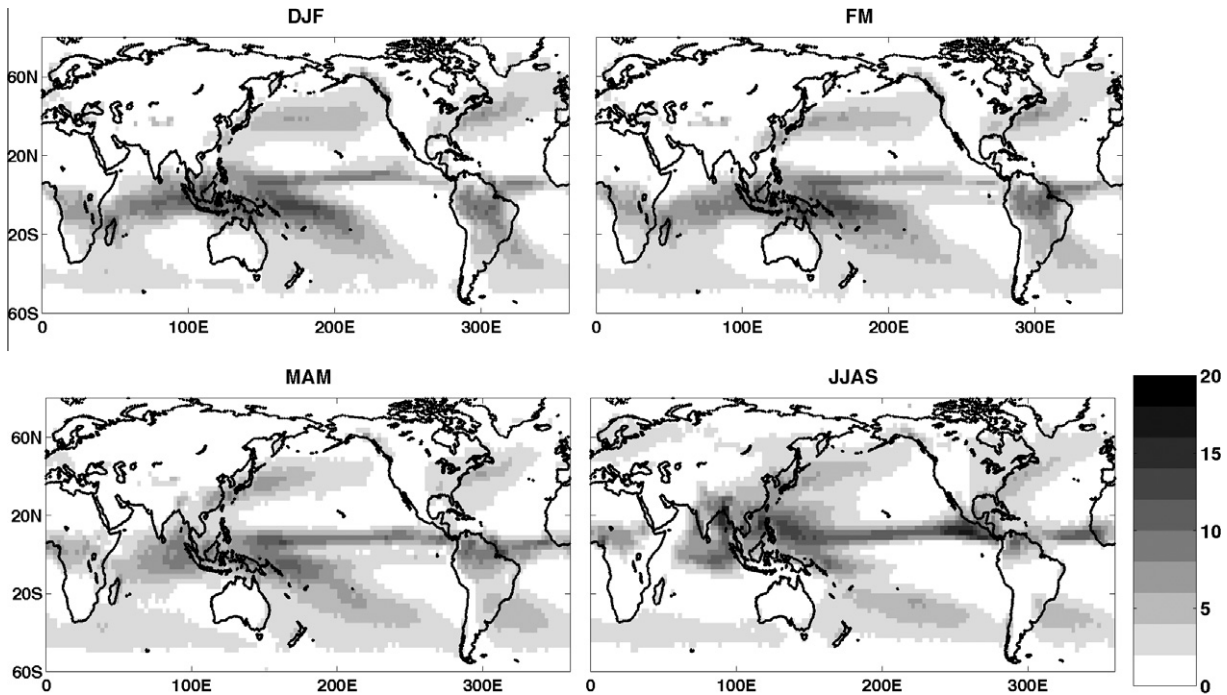


Fig. 6. Climatology of global seasonal precipitation (mm/day) (CMAP).

flow to some extent. JJAS flow is predominantly contributed by summer monsoon rainfall as well as snow and glacier melt from the upper elevations.

Observed hydro-climatic data, including daily total inflow data of Bhakra dam (1963–2004), daily-accumulated snow data at 12 stations (1976–2006), daily-rainfall data at 15 stations (1977–2006), daily maximum temperature data at 5 stations (1983–2005) and daily minimum temperature data at 2 stations were procured from the Bhakra Beas Management Board (BBMB) of India. The meteorological station information is shown in Table 1 and also shown in Fig. 1, which indicate that the snow stations are located primarily in the upper elevations. Since Satluj River

started receiving additional volume of flow through the Beas Satluj Link (BSL) channel from the late 1977, a step change occurred in the Bhakra inflow volume from 1978 onwards. Fig. 2a shows a contour plot (years in x axis, days in y axis and volume of flow in cfs in the z axis) of daily volume of inflow from Jan 1st 1963 to 31st Dec 2004 displaying the seasonality. The figure shows that the daily flow starts increasing from spring (61–155th Julian day in Fig. 2a) and in JJAS the total flow volume is the highest (156–280th Julian day in a year). Fig. 2a also shows a spread (increase) in flow volume (i.e. step change due to BSL diversion) from 1978 onwards when all the seasons start receiving higher amount of flow. This jump is also evident in the seasonal total flow time series

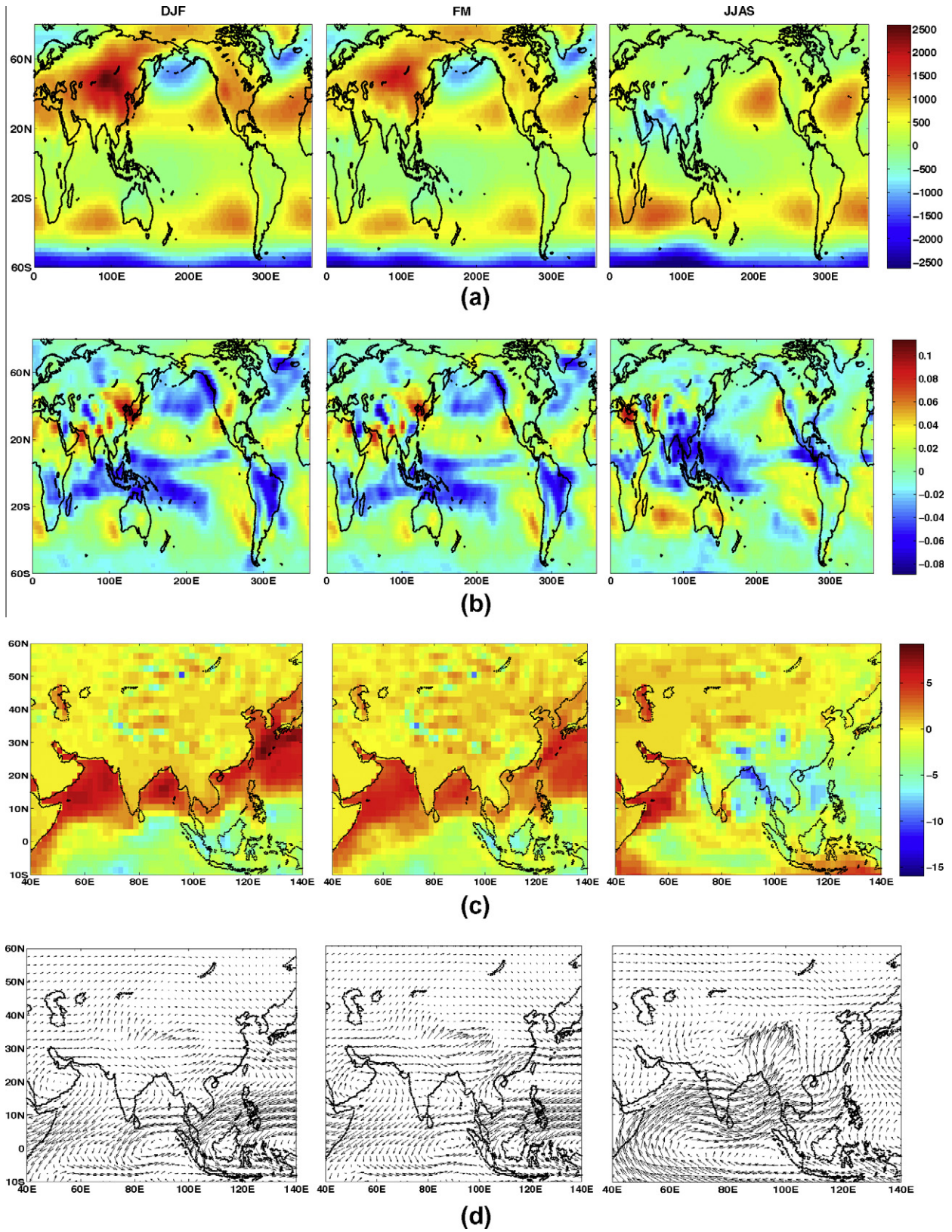


Fig. 7. Climatology of (a) mean sea level pressure (MSLP); (b) vertical motion at 500 h Pa height (ω); (c) latent heat flux (evaporation–precipitation); and (d) integrated moisture flux at 500–1000 h Pa height (data: NCEP/NCAR reanalysis 1).

shown separately in Fig. 2b. Fig. 2 as a whole indicates that JJAS is the highest flow season, which is followed by MAM – both of which is considered in this study. Due to the step jump since 1978 we considered the total inflow of Bhakra from 1978 to 2004.

Since station temperature data was available only since 1983 and also had poor spatial coverage (few stations in low elevations as in Table 1), we compared this data with the data available from other sources, especially the data from the Indian Meteorological

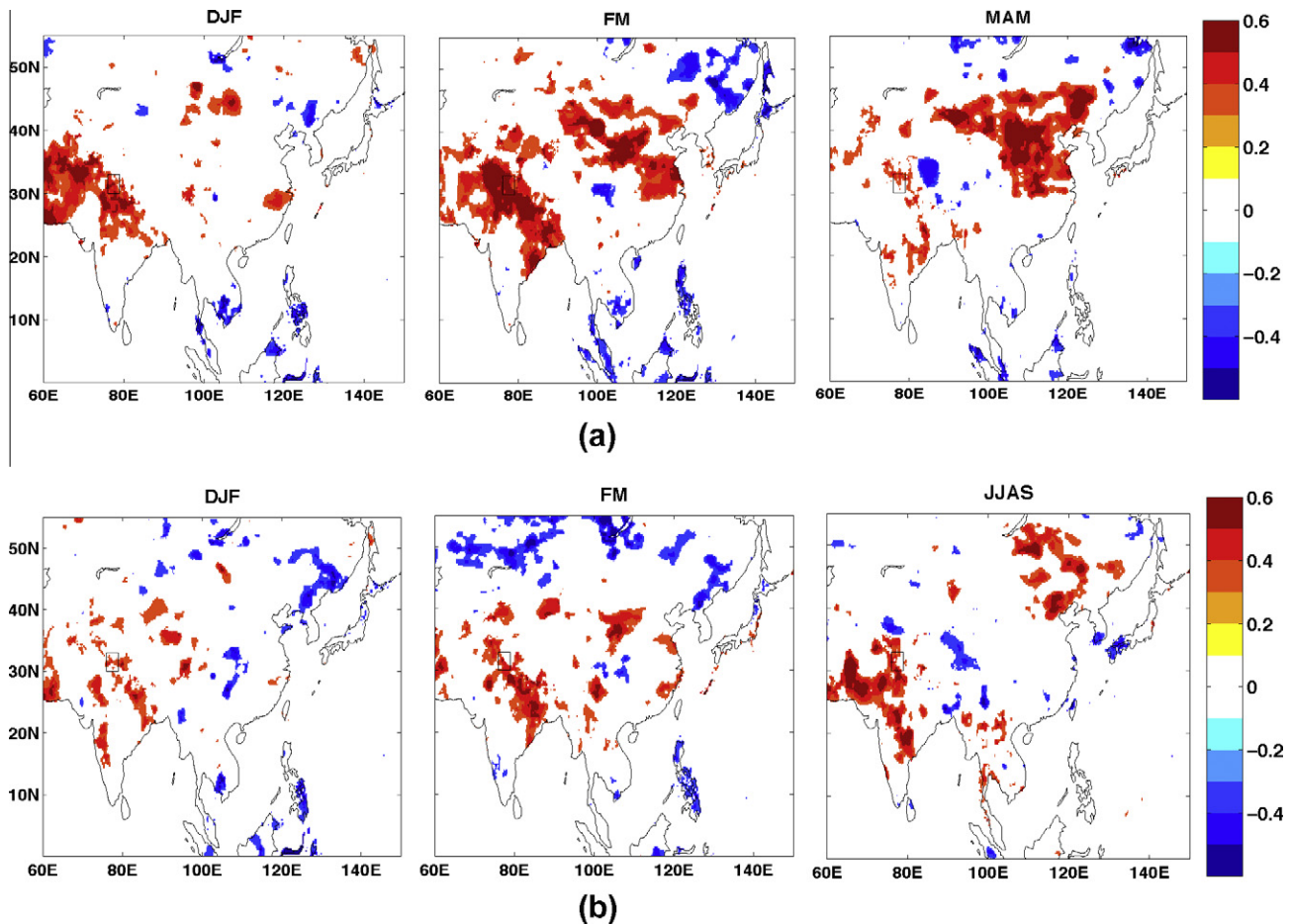


Fig. 8. Anomaly correlations (Pearson) of seasonal inflow and seasonal precipitation (a) MAM and (b) JJAS (only 95% significant regions are shown in color). (For interpretation of the references to color in this figure legend, the reader is referred to the web version of this article.)

Department (IMD) (Srivastava et al., 2008). The IMD data is gridded but they were derived using local station observations (Srivastava et al., 2008). Therefore a comparison of average data across all the stations and grids covering the Satluj river basin (30–33N and 76–79E) was carried out. Averaging temperature and precipitation data across all the stations is important, especially in winter, since the records might show large variability due to highly variable land use and topography in the Himalayas (Dimri and Das, 2012). The comparison of station temperature data with the Indian Meteorological Department (IMD) 1-degree gridded daily temperature data (Srivastava et al., 2008) for the Satluj basin indicated that they have similar climatological variability at monthly time scales for the study region (Fig. 3). Therefore, given the longer period of record (1969–2004) and better spatial coverage, IMD gridded temperature data were used whenever needed, which was averaged spatially for the Indian part of Satluj basin (30–33N and 76–79E). In addition, IMD rainfall data (Rajeevan et al., 2005, 2006) was also found to be having a good spatial and temporal (1-degree, daily) coverage for the lower elevation basin region and pose a similar variability with the spatially average station data (Fig. 3 first panel). Therefore we also used 1-degree, daily IMD rainfall data for the basin hydro-climatic studies. We determined average temperature (T_{avg}) and diurnal temperature range (DTR) by averaging T_{max} and T_{min} , and subtracting T_{min} from T_{max} on a daily basis.

Fig. 4 shows monthly climatology of the inflow and area-average rainfall, snow, average temperature (T_{avg}) and diurnal temperature range (DTR). The climatology is determined over 1978–2004. T_{max} and T_{min} were similar to T_{avg} – so not shown in Fig. 4. The

figure suggests that the basin snow and rainfall (IMD) patterns are masked by each other in different seasons and that the flow starts increasing continuously from February relative to the increase in temperature. We calculated area-average seasonal hydro-meteorological data anomalies for DJF, FM, MAM and JJAS. In addition to the traditional seasons, late winter months FM was also used because FM precipitation anomalies were found having the highest correlation with MAM and JJAS flow anomalies, which will be discussed later.

For large-scale climatological and air circulation patterns linked to MAM and JJAS flow anomalies we used APHRODITE (Yatagai et al., 2009), CPC Merged Analysis of precipitation (CMAP) (Xie and Arkin, 1996, 1997) and NCEP/NCAR reanalysis V1.0 monthly products (Kalnay et al., 1996) from 1978 to 2004 (CMAP was available from 1979). APHRODITE is a suite of precipitation products (version: V0902), which are constructed by the Asian Precipitation Highly Resolved Observational Data Integration Towards Evaluation of the Water Resources (APHRODITE's water resources) project in collaboration of Research Institute for Humanity and Nature and Meteorological Research Institute of Japan Meteorological Agency. The product is 0.5×0.5 and $0.25 \times 0.25^\circ$ gridded data over Monsoon Asia, Russia, and Middle East. We used $0.25 \times 0.25^\circ$ gridded precipitation data over Monsoon Asia. Since APHRODITE precipitation dataset is primarily land based, we also used standard global gridded (2.5°) monthly estimated precipitation product (CMAP) for the analysis of oceanic precipitation. This data was available from NOAA NCEP CPC. We used latest version 2 that used rain gauge and satellite estimates to develop the dataset. We

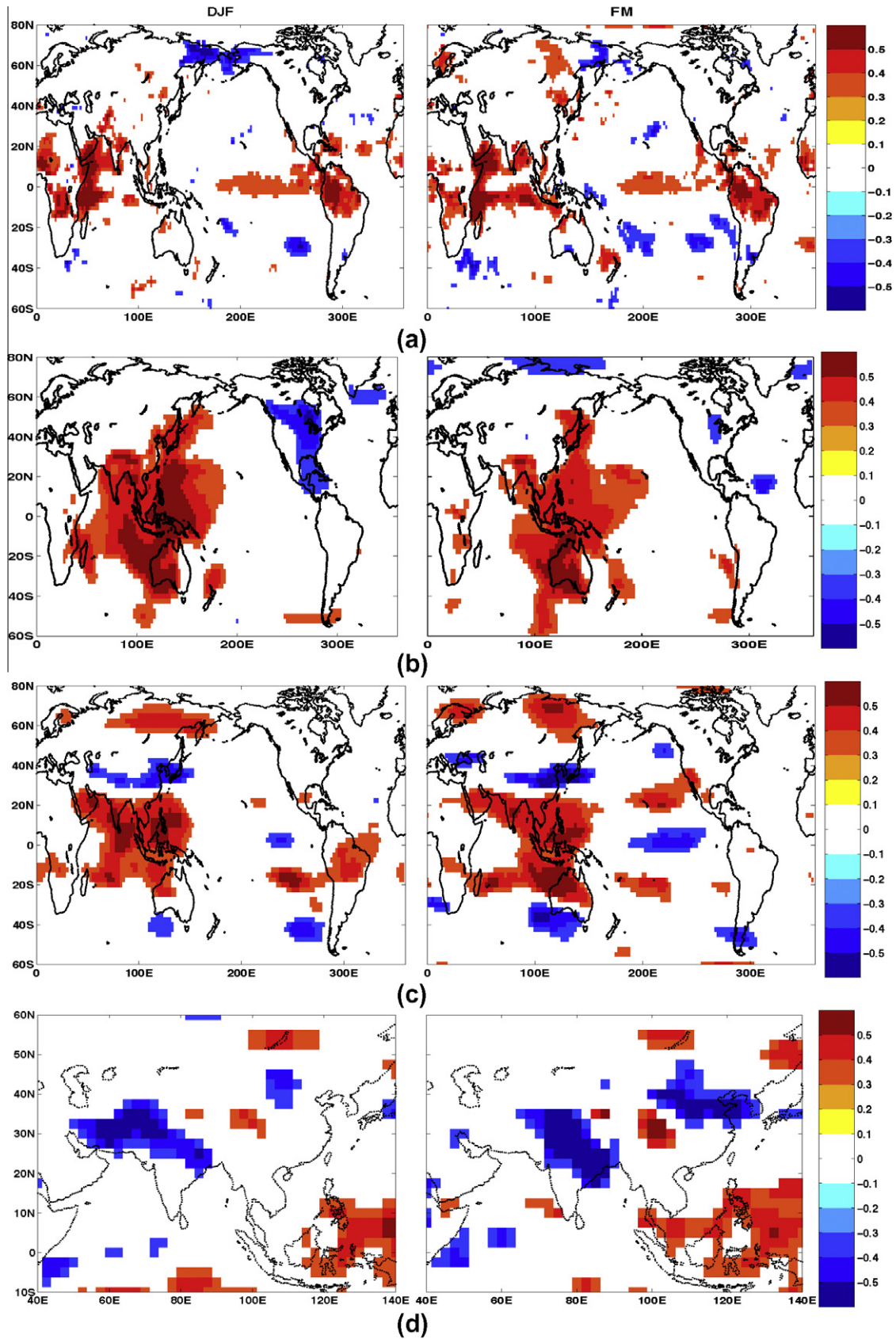


Fig. 9. Anomaly correlations (Pearson) of MAM inflow and seasonal climatological and air circulation parameters (a) surface temperature; (b) mean sea level pressure (MSLP); (c) zonal wind at 200 h Pa height (u200); and (d) vertical motion at 500 h Pa height (omega) (only 95% significant regions are shown in color). (For interpretation of the references to color in this figure legend, the reader is referred to the web version of this article.)

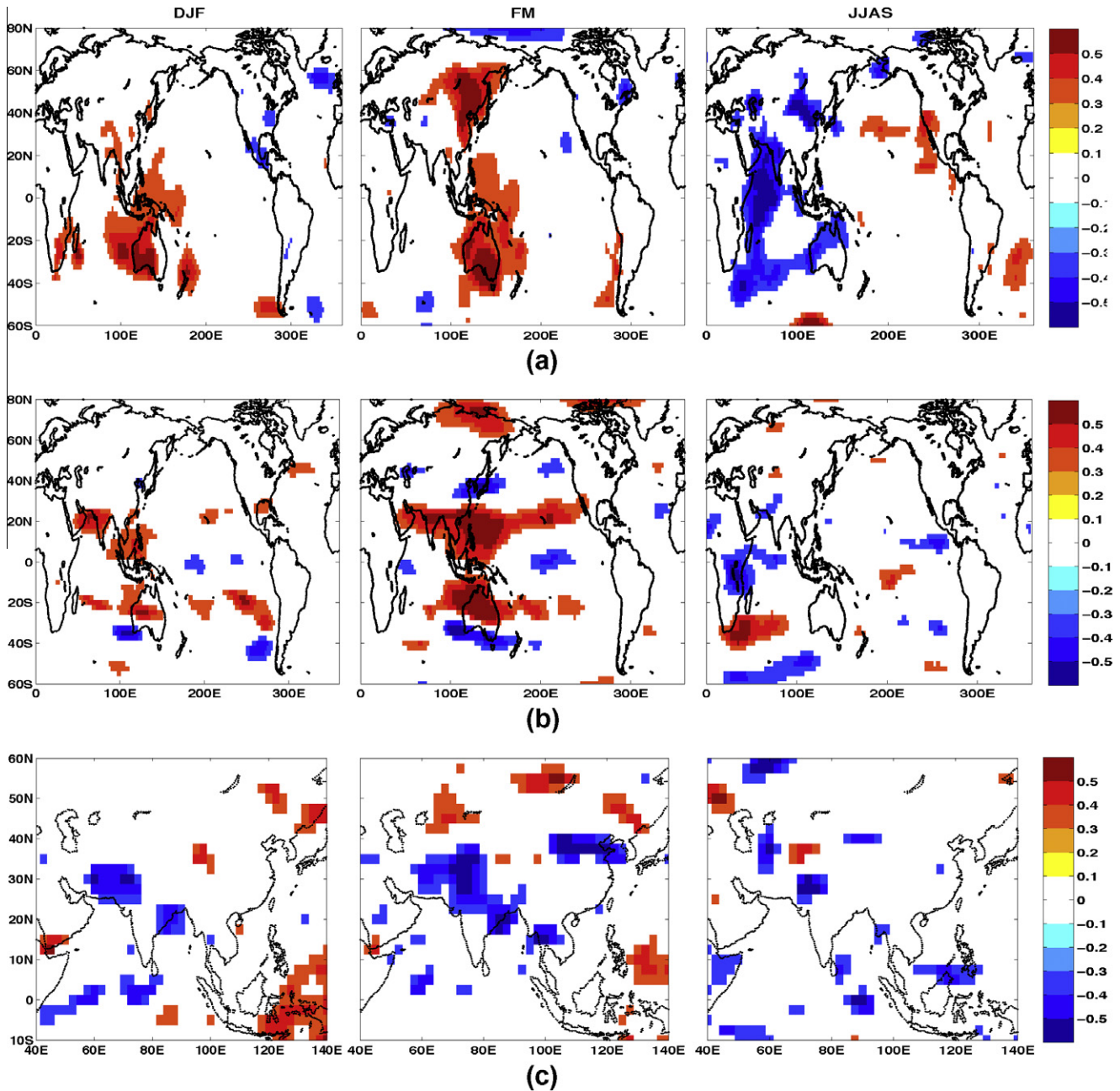


Fig. 10. Anomaly correlations (Pearson) of JJAS inflow and seasonal climatological and air circulation parameters (a) mean sea level pressure (MSLP); (b) zonal wind at 200 h Pa height (u_{200}); and (c) vertical motion at 500 h Pa height (ω) (only 95% significant regions are shown in color). (For interpretation of the references to color in this figure legend, the reader is referred to the web version of this article.)

downloaded all the above datasets from the IRI data library (<http://www.irdl.ldeo.columbia.edu/>).

The seasonal climatology (mean over all the years in mm/season) of precipitation data (APHRODITE) for DJF, FM, MAM and JJAS are shown in Fig. 5. The figure shows that the Satluj basin (marked in a small black box in Fig. 5a and also shown enlarged in b) receives about the same range of precipitation in total in FM and DJF while MAM is higher than both DJF and FM in the same region. The maximum precipitation in MAM is in the north. JJAS precipitation is the highest but the maximum precipitation region in the basin is located differently compared to MAM season, more concentrated at the northwest and southeast of the basin. Fig. 6 depicts the seasonal climatology (in mm/day) of global precipitation data (CMAP), which indicates highest amount of precipitation over the oceans in all the seasons.

We carried out a detailed correlation analysis of MAM and JJAS inflow versus area-average meteorological parameters. A correlation analysis indicates important co-bearing between 2 parameters, which might not necessarily explain the cause-effect relationships because the hydro-climatic system is a complex dynamical system. However, since there is limited knowledge on the physical mechanisms underlying how the large-scale climatic variability influences the hydrology of the study region and Western Himalayas, this research makes a useful step forward.

We found that MAM flow is positively and significantly correlated with snow in concurrent season (Pearson correlation coefficient value = +0.63), which is also true for DJF precipitation but the correlation is much weaker (Pearson correlation value for rainfall = +0.39 and snow = 0.32; as in Pal et al., 2012). The correlation with snow in MAM is much higher than the rainfall (+0.35). MAM

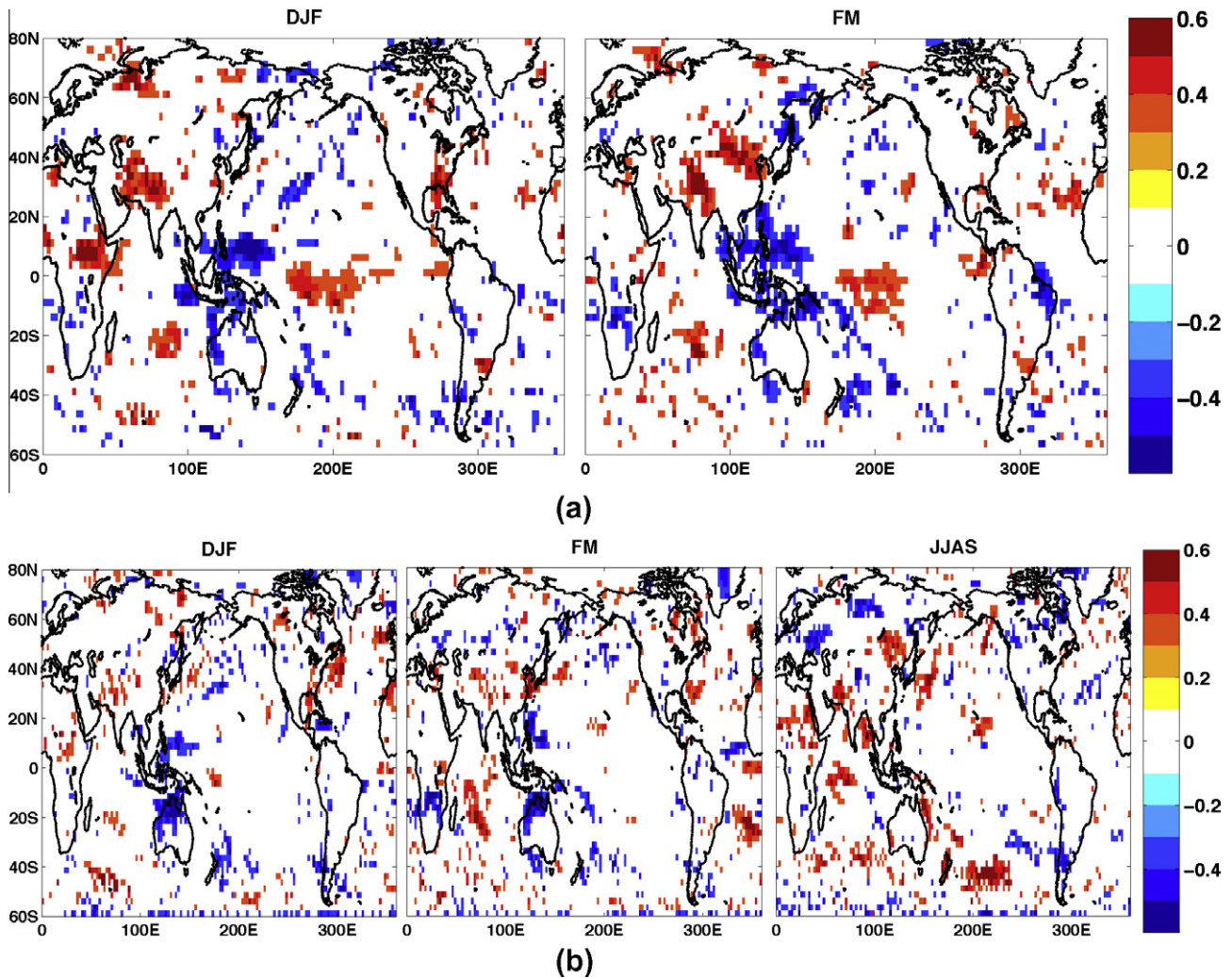


Fig. 11. Anomaly correlations (Pearson) of seasonal inflow and seasonal global precipitation (CMAP) (a) MAM and (b) JJAS (only 95% significant regions are shown in color). (For interpretation of the references to color in this figure legend, the reader is referred to the web version of this article.)

flow negatively correlates with temperature in the concurrent season, which is not significant. However, it significantly negatively correlates with DTR and T_{\max} in DJF (-0.57 and -0.37 respectively). Therefore, basin level DJF rainfall and temperature (T_{\max} and DTR) might be used as potential predictors of MAM flow with some lead time while average snow in MAM relates more with the flow amount (Pal et al., 2012). A more detailed analysis indicated that MAM flow has the highest and significant correlation with average FM climatology – which is positive with rainfall (0.60) and snow (0.72); and negative with DTR (-0.76), T_{\max} (-0.57) and T_{avg} (-0.43). We also found that only February or March climatology individually correlates with MAM flow to a great extent. For example we found positive and significant correlation of MAM flow and February rainfall (0.61) and snow (0.46), and negative correlation with DTR (-0.70) and T_{\max} (-0.41). On the other hand, we found positive and significant correlation of MAM flow and March rainfall (0.50) and snow (0.63); and negative correlation with March DTR (-0.67), T_{\max} (-0.55) and T_{avg} (-0.48). The individual monthly analyses indicated that while February climatology is important to consider for predicting MAM flow, it correlates best with the FM average conditions.

On the other hand, interestingly, JJA average flow is not correlated with concurrent precipitation or temperature, but positively and significantly correlated with snow (0.54) and T_{\min} (-0.40) in MAM season. A more detailed analysis found that a higher correla-

tion exists between average flow in JJ (June and July) and snow in MA (March–April) (0.59). JJ flow was also significantly correlated with FM/M snow (0.47) and F rainfall (0.61). Since JJ flow is contributed partly by snow and glacier melts, average JJAS flow was found to be significantly and positively correlated with FM rainfall (0.54) as well. SON flow is also significantly correlated with SON rainfall (0.64).

The above correlation analysis indicated that DJF and FM climatological conditions might be the important drivers for MAM flow. On the other hand, although JJAS precipitation is partly contributed by FM snow/ice melt as well as JJAS rainfall by summer monsoon, we looked at large scale climatological and atmospheric conditions in DJF, FM and JJAS seasons. This diagnostic study will be useful to understand the large-scale climatological parameters affecting Western Himalayan hydro-climatology that is useful for improving the long-lead prediction studies of river flow in different seasons.

Fig. 7 shows DJF, FM and JJAS climatology of (a) mean sea level pressure (MSLP), (b) vertical motion at 500 h Pa height (Omega), (c) differences in evaporation and precipitation rates (E–P), and (d) integrated moisture flux (specific humidity \times zonal/meridional wind – integrated over 500 h Pa to 1000 h Pa heights). The data shown in Fig. 7 are the anomalies with large-scale spatial mean removed. Generally a high-pressure system prevails over Siberia in DJF that extends up to northern India, as in Fig. 7a. This high-pressure system subsides in FM. JJAS MSLP conditions are different

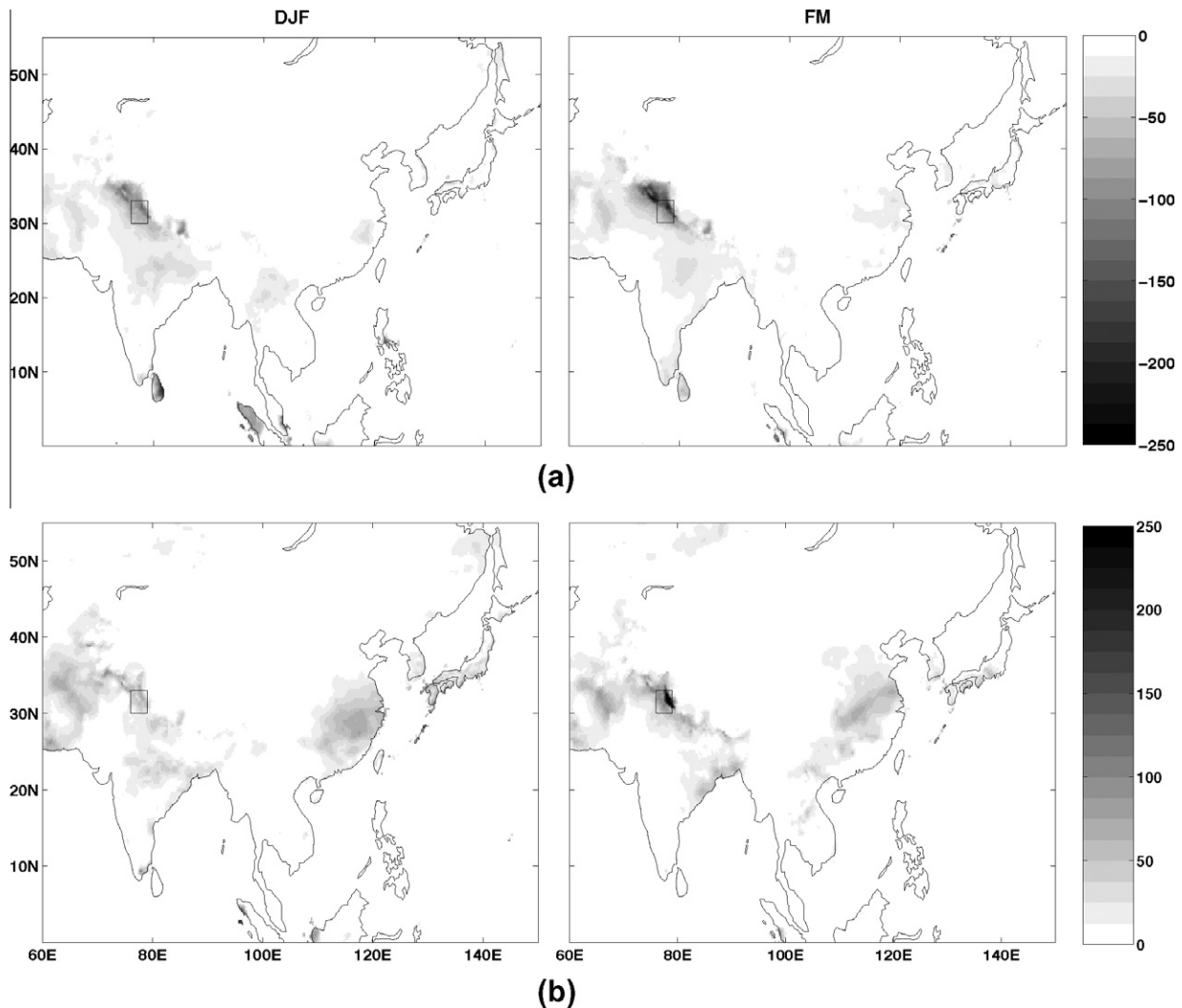


Fig. 12. Anomaly composites of low and high MAM inflow and seasonal precipitation anomalies – (a) low flow and (b) high flow.

with a low-pressure anomaly over the Indian sub-continent and higher-pressure system over southern Indian Ocean that is enhanced from the other two seasons (Fig. 7a). 500 h Pa vertical velocity (Ω) indicates regions of rising (blue) and sinking (red) motions. 500 h Pa vertical motion also provides a nice diagnostics of the primary rain areas. If we compare Figs. 5a, 6 and 7b we understand that there are negative vertical motion or lift over the Western Himalayas, Saudi Arabia and maritime continents in DJF and FM, and over the west coast of peninsular India, north-eastern India and south-east Asia as a whole in JJAS during summer monsoon. This also holds true for the oceanic regions in all the seasons (Figs. 6 and 7b). Fig. 7c shows climatology of the differences between evaporation (latent heat) and precipitation rates (E–P). Red indicates more evaporation and blue indicates more precipitation. As the figure suggests, Western Himalayas experience more precipitation than evaporation in DJF and FM but evaporation rate is high over the Arabian Sea, western Indian Ocean and the Bay of Bengal at the same time. On the other hand precipitation rate is higher than evaporation due to summer monsoon in JJAS over the western coast of peninsular India and northeastern India – the usual higher monsoon rainfall regions of India. At the same time the evaporation is high over the western parts of Arabian Sea and Indian Oceans. Interestingly, the Bay of Bengal shows more precipitation than evaporation in JJAS. Fig. 7d shows climatology of integrated moisture flux in DJF, FM and JJAS. We notice that south-

westerly flux brings moisture in DJF and FM to northwest India and the study region across the Arabian Peninsula mainly from the Arabian Sea and tropical Africa-ITCZ region. On the other hand, southwesterly flux also brings moisture from the Indian Ocean and Arabian Sea to Indian Subcontinent and Southeast Asia in JJAS, which follow a different route. In DJF and FM the moisture flux activities are similar to each other. We also noticed northeast (winter) monsoon activities over maritime continents in DJF and FM, as there are high moisture fluxes over the Western Pacific ocean.

3. Results and discussions

Regional precipitation over the Satluj River basin in the Western Himalayas responds to large-scale circulation patterns. We explore these spatial patterns through simple Pearson correlations and composite analyses. The correlation analyses results are shown in Figs. 8–11. The color scales in those figures indicate correlation coefficient values. To maintain consistency, the scales are kept from -0.6 to $+0.6$ but sometimes the values did cross these upper and lower bounds, which are mentioned in the text below. The correlation and composite analyses will help us to identify the possibility for downscaling climate change or seasonal climate forecasts, and/or to explore how trends in circulation patterns relate to trends in surface meteorological/climatological variables and total river flow into Bhakra.

3.1. Spatial correlation patterns of large scale climatology and atmospheric circulation linked with Bhakra reservoir inflow anomalies

Bhakra inflow anomalies in MAM are not only positively correlated with precipitation anomalies in DJF (max spatial correlation coefficient = 0.70) and FM (max spatial correlation coefficient = 0.80) over the northwest and northern India, but also with southern Pakistan, as indicated in Fig. 8a. Correlations become somewhat stronger in FM with significantly correlated region moves little eastwards. The correlation of MAM flow with concurrent rainfall is very weak over north India but positive significant correlation is still noticed over the study region (small box marked in the correlation maps in Fig. 8a). Interestingly, MAM precipitation over Siberian region is highly and positively correlated with MAM flow. On the other hand JJAS flow anomaly is also positively correlated with precipitation in DJF (max spatial correlation coefficient = 0.61) and FM (max spatial correlation coefficient = 0.66) over northern India while correlation with FM precipitation is higher and concentrated more over the northeast India, as in Fig. 8b. The correlation of JJAS flow with concurrent precipitation anomaly is strong over northwest India but lower and positive significant correlation is noticed over the study region (max spatial correlation coefficient = 0.71).

MAM Bhakra inflow is positively correlated with the SSTs over the equatorial western Indian Ocean and Arabian Sea adjacent to the Somalia and Saudi Arabian coasts, and equatorial central Pacific, though weaker (max spatial correlation coefficient noticed was > 0.70), as shown in Fig. 9a. This positive significant correlation with central Pacific SST or ENSO like pattern in DJF is consistent with the finding of Mariotti (2007), who demonstrated that a linkage exists between warm phase of ENSO and enhanced precipitation over southwest central Asia region while Barlow and

Tippet (2008) also reported a relatively stronger signal in the central rather than eastern Pacific. The positive significant anomaly correlations with the SST over southern Arabian Sea, as noticed in Fig. 9a, is related to the positive significant anomaly correlations over western Indian Ocean SST (Vinayachandran and Kurian, 2008). These results also support the fact that winter (DJF) rainfall over southwest Asia and particularly the northwest India fluctuates with winter SSTs over the equatorial Indian Ocean and central Pacific, and winter MSLP over eastern tropical Hemisphere (Barlow et al., 2007; Yadav et al., 2010) that is consistent with Fig. 9b (max spatial correlation coefficient ~ 0.60). This translates into the significant correlation between DJF SST and MSLP fields versus Satluj basin rainfall and snow as well since the same climate mechanism causes precipitation in these regions (not shown). In addition, the large-scale high-pressure anomaly over the Indian and western Pacific Oceans i.e. western pole of the Southern Oscillation sea-saw pattern, as seen here correlate to MAM flow (Fig. 9b) was also found linked with DJF/FM precipitation brought by southwesterly moisture flux to southwest central Asia (Mariotti, 2007). The same authors also reported that the role of Indian Ocean SST anomalies counters the Pacific influence to winter precipitation over this region. Fig. 9c shows that MAM flow is positively correlated with upper level 200 h Pa zonal wind in DJF and FM over Arabian Sea, tropical Indian Ocean and maritime continents (max spatial correlation coefficient ~ 0.60). MAM flow is also negatively correlated with 500 h Pa vertical motion, which is an indication of precipitation activity (Fig. 9d), in DJF and FM over northern India and Pakistan, which is also evident in Figs. 8a and 11a. Fig. 11 depicts the anomaly correlations between MAM and JJAS flow and global precipitation that includes ocean precipitation as well unlike Fig. 8. Significant correlation region for 500 h Pa vertical motion in FM also moves eastward, like precipitation in Figs. 8a and 11a

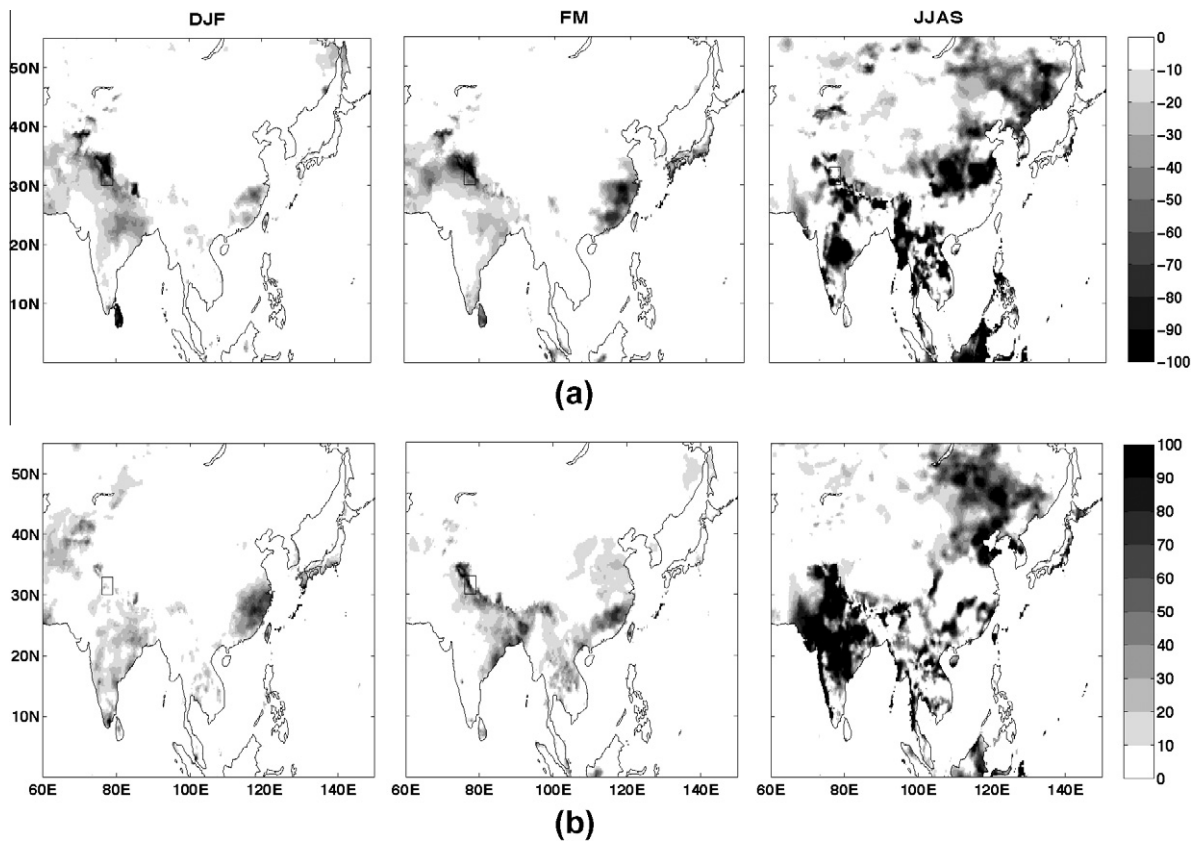


Fig. 13. Anomaly composites of low and high JJAS inflow and seasonal precipitation anomalies – (a) low flow and (b) high flow.

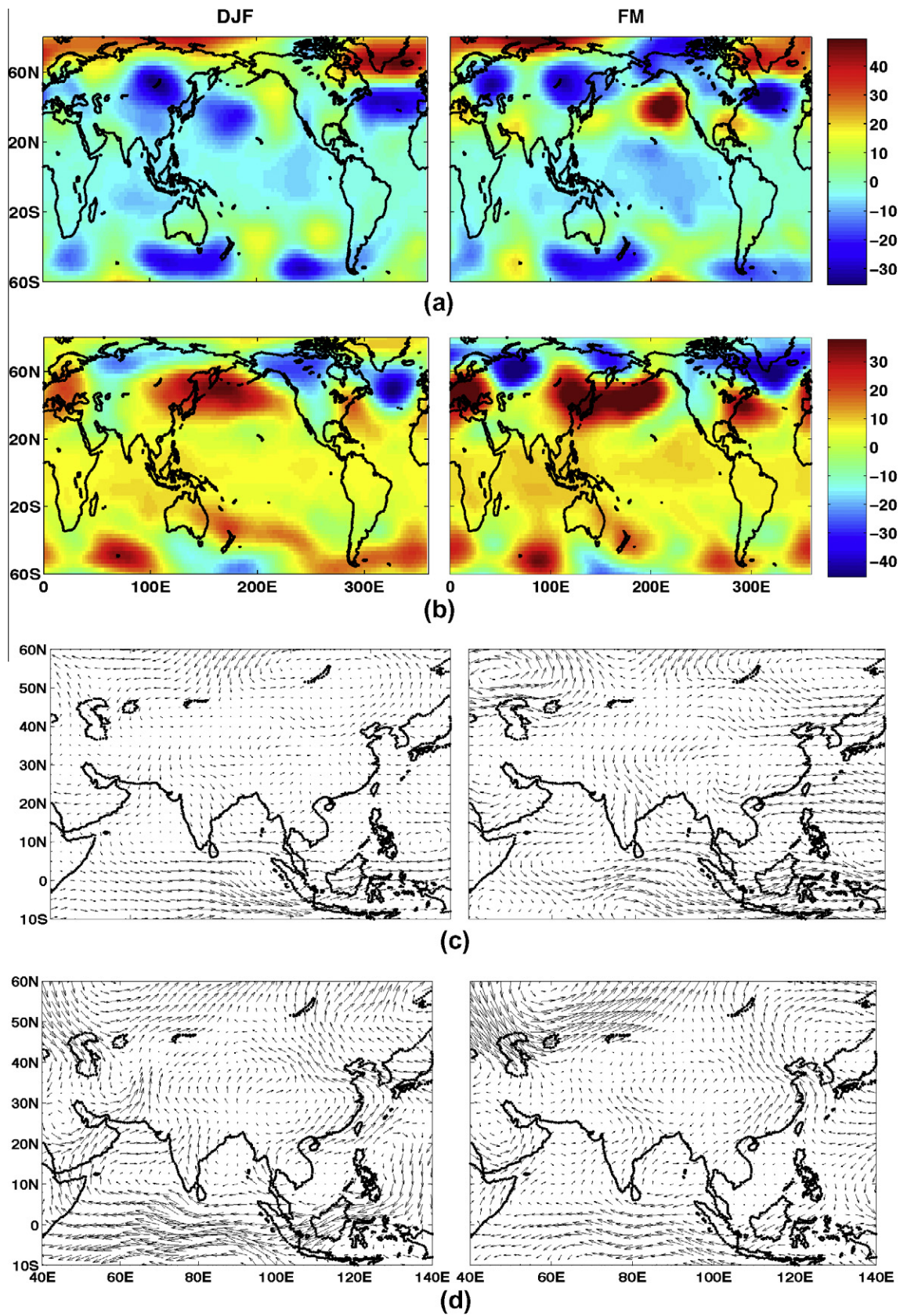


Fig. 14. Anomaly composites of low and high MAM inflow and seasonal atmospheric circulation patterns (a) low flow and Z500; (b) high flow and Z500; (c) low flow and 850 h Pa wind vector; and (d) high flow and 850 h Pa wind vector.

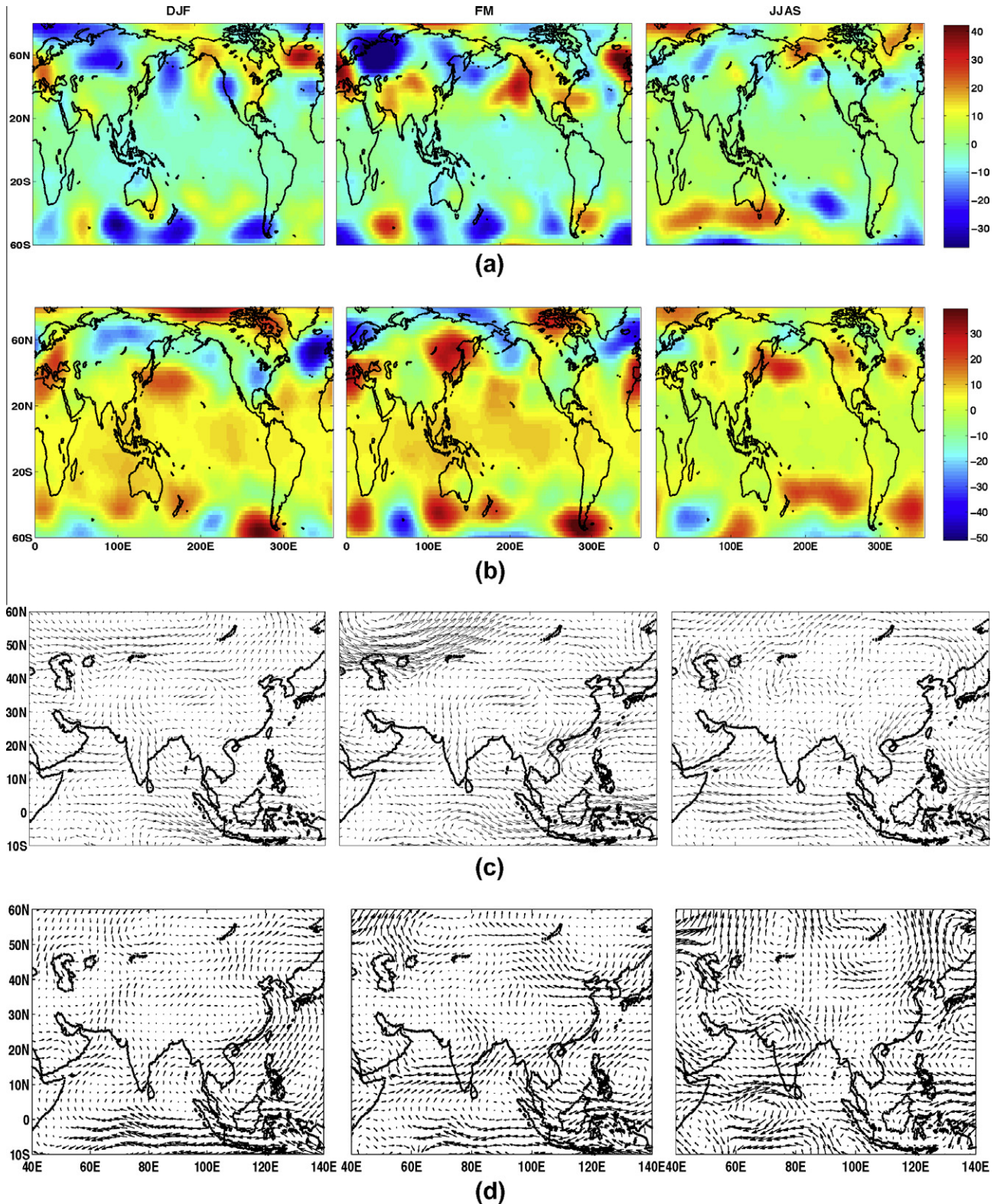


Fig. 15. Anomaly composites of low and high JJAS inflow and seasonal atmospheric circulation patterns (a) low flow and Z500; (b) high flow and Z500; (c) low flow and 850 h Pa wind vector; and (d) high flow and 850 h Pa wind vector.

(max negative spatial correlation coefficient in Fig. 9d = -0.76 in FM). Precipitation over the Maritime continents negatively correlates with MAM flow, as seen in Fig. 9d and also verified in Fig. 11a.

Significance of the anomaly correlations of JJAS Bhakra inflow and SSTs were very low and therefore not shown. Fig. 10a shows positive significant anomaly correlations between JJAS flow and

MSLP over the maritime continents in DJF and FM (max spatial correlation coefficient = -0.72 in FM). These correlation fields are not as strong as noticed for MAM flow in Fig. 9b. JJAS flow is negatively correlated with MSLP over western and southern Indian Ocean, whole Arabian Sea, and Indian subcontinent, which mean that low pressure over this region is the key for JJAS precipitation. JJAS

river flow is positively correlated with DJF zonal wind at 200 h Pa height over the northern Arabian Sea and peninsular Indian sub-continent while the significant correlation field gets bigger for FM u200 (Fig. 10b). The correlation patterns of JJAS flow and JJAS u200 is weak but negative significant correlation was noticed for northwest India (maximum negative correlation coefficient in FM = -0.59). Since positive zonal wind means direction of the wind from west to east, i.e. westerly, JJAS and MAM flow is positively correlated with westerly wind in DJF and FM over northern India while the wind direction changes during JJAS, as also noticed in Fig. 7d. Like MAM in Fig. 9d JJAS flow was also found to be having negative significant correlation with vertical motion anomalies at 500 h Pa over northern India (Fig. 10c), which directly relates to precipitation as also verified in Fig. 11b like MAM (max negative correlation coefficient in DJF in Fig. 10c = -0.68 , and in FM = -0.64). On the other hand, JJAS flow is negatively correlated with vertical motion in JJAS in northwest India (max negative correlation coefficient in JJAS = -0.62) and positively correlated with precipitation (Fig. 11b).

3.2. Low/high inflow composites with large-scale climatology and circulation patterns

Composite analyses are helpful to understand the differences between the large-scale climatological/atmospheric patterns associated with low or high volume of flow or precipitation. The MAM/JJAS inflow volumes those are \pm one standard deviation of long term (1978–2004) flow climatology was categorized as high and low flow respectively. In other words, low (high) flow seasons are those seasons when lower (greater) than one standard deviation of flow anomaly occurred. High/low MAM/JJAS inflow volume was a result of high/low precipitation as a result of changing circulation patterns. After determining the years, which had low/high inflow, we defined climatology and atmospheric circulation patterns averaged across those low/high flow years to study the distinct conditions, which are called composites. Since number of years corresponding to low/high inflow is small, the results discussed here are more indicative than conclusive.

Fig. 12 shows low and high MAM flow composites with seasonal precipitation anomalies. As expected, low (high) flow years received negative (positive) precipitation anomalies in both DJF and FM, while the composites in FM are concentrated in the study region and DJF showed similar anomalies over northern India and Pakistan. On the other hand, Fig. 13 shows that low (high) JJAS flow years generally receive low (high) precipitation in DJF, FM as well as JJAS, while JJAS is concentrated in the monsoonal regions in India that includes the study region as well.

Low MAM flow in a year is on an average associated with positive 500 h Pa geopotential height (Z500) anomaly over the Arctic, negative Z500 over Siberia/eastern Russia, northwest Pacific Ocean and south of Australia over the Southern Ocean in DJF, as in Fig. 14a. This circulation parameter changes in FM for a low flow year. While negative Z500 still maintains over Siberia, another negative Z500 zone develops over western Russia and two positive Z500 anomaly zones built up over northwest India and Mediterranean Sea respectively (Fig. 14a). Negative Z500 anomaly region prevails over the North Atlantic Ocean both in DJF and FM in the low flow years. High flow and Z500 composites were different than low flow. A large high-pressure region (positive Z500) with center over the northwest Pacific extends until Japan and northern China and Mongolia in DJF, which enhances in FM, as seen in Fig. 14b. Another high-pressure region (positive Z500) builds up in DJF and enhances in FM over Eastern Europe. On the other hand, a low-pressure system stays east of Northern Europe extending south all the way until northwest India and Pakistan. While negative Z500 in DJF over North Atlantic remains in high flow years, the

location of the center of the same moves further north and a positive Z500 zone develops in FM over eastern North America, as in Fig. 14b.

Fig. 14c and d shows low-level average wind vectors (uv850) expected in low and high MAM flow years respectively. We found DJF 850 h Pa wind vectors directing from northwest India and Pakistan towards Arabian Sea and Peninsular India before drifting towards Saudi Arabia and Maritime continents respectively in low flow years. This is also true for FM wind vector but the magnitudes of the wind vectors are more pronounced in FM for both the branches of winds mentioned above. West to eastwards wind activity was also noted over southern Indian Ocean in low flow years. The wind activities change in the high flow years, as in Fig. 14d. We found that the direction of wind vector is from the east to western Indian Ocean via the horn of Africa to Saudi Arabia to northwest India and Pakistan in high flow years. A part of it also goes through Arabian Sea to Peninsular India to north India. In FM, the wind convergence at northwest India and Pakistan is similar to DJF in a high flow year but higher wind activity is observed over the Western Russia and Caspian Sea in FM. In high flow years, the wind activity is lower over the Maritime continent in FM as compared to DJF but in a low flow year that becomes the opposite.

Low JJAS flow years on an average are associated with positive Z500 regions over the Eastern Europe and northwest India, and negative Z500 regions over central Russia and northwest Pacific Ocean in DJF, as in Fig. 15a. In FM, all those anomalous regions are found enhanced for low JJAS flow conditions. In JJAS nothing significant happens with Z500 over India or nearby regions but a positive Z500 system prevails over the Southern Ocean. In high JJAS flow years, negative (but weak) anomalous Z500 persists from Russia to entire Northern Pacific and North America in DJF. In FM, that negative Z500 anomaly region shifts northwards, two positive Z500 anomaly regions prevail over Eastern Europe (over the Mediterranean sea) and eastern Russia but a weak low pressure region sweeps within them all the way until north India, as in Fig. 15b. In high JJAS flow years no significant patterns are noted for JJAS Z500 except a positive Z500 region over western North Pacific and a pressure dipole over Southern Ocean, although that was found more enhanced in FM.

Fig. 15c and d shows low-level average wind vectors (uv850) expected in low and high JJAS flow years respectively. Like MAM, we found DJF 850 h Pa wind vectors are directed from northwest India and Pakistan towards Arabian Sea and Peninsular India before drifting towards Saudi Arabia and Maritime continents respectively. This is also true for FM wind vectors with some additional enhanced wind activities noted over the western Russia and north of Caspian Sea. In JJAS a convergence of wind vectors noted over Caspian sea in low flow years but the convergence occurs over northwest India in a high flow year (Fig. 15c and d). A convergence zone is also noted at the south of India over the India Ocean in JJAS in high flow years. In addition, in typical low JJAS flow years wind vectors have lower magnitude as compared to high flow years.

4. Summary

This study looked at the annual variability and links of MAM and JJAS Bhakra reservoir inflow across Satluj River that originates from the Western Himalayas and flows over the northwestern plains of India. The analyses were based on the Pearson anomaly correlations and anomaly composites using observed and reanalysis climatology and air circulation fields procured from different data sources for 1978–2004. We have found that the volume of inflow of Bhakra reservoir in MAM season is strongly correlated with DJF and FM precipitation (and temperature) over the Satluj River basin, which is linked with the concurrent SST conditions over western Indian Ocean and Arabian Sea. Therefore, MAM flow

anomalies were also found to be linked with large scale air circulation patterns governed by the SST and MSLP fields around Indian and Pacific Oceans in DJF and FM. Volume of JJAS inflow of Bhakra reservoir, which contributes to 66% of annual total flow, was also found to be correlated with FM precipitation (and temperature) over the Satluj River basin and circulation parameters both in FM and JJAS seasons. JJAS flow was found to be correlating both with FM and JJAS air circulation parameters indicating a mixture of snow melts contribution that deposits in the previous season as well as summer monsoon rain.

Composite analyses of high and low flow indicated that they are directly linked with the high or low volume of precipitation over the Satluj basin, which is linked with different air circulation patterns. It was found that different geopotential height and wind conditions are associated with high and low seasonal inflow. Common high-pressure fields dominate in FM over the northwest India and Eastern Europe in low MAM and JJAS flow years. On the other hand, lower pressure system prevails over north India in FM in high JJAS flow years. These conditions lead to high convergence of moisture flux from the Arabian Sea and leading to high volume of precipitation in FM that contributes to MAM and JJAS flow (to some extent).

Taken together, the study presented here indicates that high/low spring inflow to Bhakra over Satluj River is directly connected with modulation of Western Himalayan precipitation and temperatures in winter that is remotely linked with the large-scale winter atmospheric circulations. We are at a very early stage of our understanding of regional climate variability and its impact on the river flows in the Himalayas. Since there are many large-scale climate actors in play, dynamical model experiments are needed to better diagnose the response of Western Himalayan climate and hydrology.

References

- Barlow, M.A., Tippet, M.K., 2008. Variability and predictability of central Asia river flows: antecedent winter precipitation and large-scale teleconnections. *J. Hydrometeorol.* 9, 1334–1349.
- Barlow, M.A., Hoell, A., Colby, F., 2007. Examining the wintertime response to tropical convection over the Indian Ocean by modifying convective heating in a full atmospheric model. *Geophys. Res. Lett.* 34, L19702.
- Dimri, A.P., 2005. The contrasting features of winter circulation during surplus and deficient precipitation over western Himalayas. *Pure Appl. Geophys.* 162, 2215–2237.
- Dimri, A.P., 2006. Surface and upper air fields during extreme winter precipitation over the western Himalayas. *Pure Appl. Geophys.* 163, 1679–1698.
- Dimri, A.P., 2007. The transport of momentum, sensible heat, potential energy and moisture over the western Himalayas during the winter season. *Theor. Appl. Climatol.* 90, 49–63.
- Dimri, A.P., Dash, S.K., 2012. Wintertime Climatic Trends in the Western Himalayas. *Climatic Change* 111 (3–4), 775–800.
- Dimri, A.P., Mohanty, U.C., Mandal, M., 2004. Simulation of heavy precipitation associated with an intense western disturbance over western Himalayas. *Nat. Hazards* 31, 499–521.
- Kalnay, E., Kanamitsu, M., Kistler, R., Collins, W., Deaven, D., Gandin, L., Iredell, M., Saha, S., White, G., Woollen, J., Zhu, Y., Leetmaa, A., Reynolds, B., Chelliah, M., Ebisuzaki, W., Higgins, W., Janowiak, J., Mo, K.C., Ropelewski, C., Wang, J., Jenne, R., Joseph, D., 1996. The NCEP/NCAR 40-Year Reanalysis Project. *Bulletin of the American Meteorological Society* March, 1996.
- Mariotti, A., 2007. How ENSO impacts precipitation in southwest central Asia. *Geophys. Res. Lett.* 34, L16706.
- Pal, I., Lall, U., Robertson, A., Cane, M., Bansal, R., 2012. Predictability of Western Himalayan river flow: melt seasonal inflow into Bhakra reservoir in northern India. *Hydrol. Earth Syst. Sci. Discuss.* 9, 8137–8172.
- Rajeevan, M., Bhate, J., Kale, J.D., Lal, B., 2005. Development of a High Resolution Daily Gridded Rainfall Data for the Indian Region. *Indian Meteorological Department, Met. Monograph Climatology No. 22/2005*, pp. 26.
- Rajeevan, M., Bhate, J., Kale, J.D., Lal, B., 2006. A high resolution daily gridded rainfall for the Indian region: analysis of break and active monsoon spells. *Curr. Sci.* 91 (3), 296–306.
- Rao, V.B., Rao, S.T., 1971. A theoretical and synoptic study of western disturbances. *Pure Appl. Geophys.* 90, 193–208.
- Sen Gupta, R., Desa, E., 2001. The Indian Ocean – a perspective. In: Balkema, A.A. (Ed.), *A Member of Swets & Zeitlinger Publishers*.
- Singh, P., Jain, S.K., 2002. Snow and glacier melt in the Satluj River at Bhakra Dam in the Western Himalayan region. *Hydrol. Sci. J.* 47 (1), 93–106.
- Singh, P., Quick, M.C., 1993. Streamflow simulation of Satluj river in the Western Himalayas. *Snow and Glacier Hydrology*. In: *Proceedings of the Kathmandu Symposium, November 2002*. IAHS Publication No. 218, pp. 261–271.
- Srivastava, A.K., Rajeevan, M., Kshirsagar, S.R., 2008. Development of a High Resolution Daily Gridded Temperature Data Set (1969–2005) for the Indian Region. *NCC Research Report 8*. National Climate Centre, India Meteorological Department, Pune 411005, India. pp. 1–18.
- Vinayachandran, P.N., Kurian, J., 2008. Modelling Indian Ocean circulation: Bay of Bengal fresh plume and Arabian Sea mini warm pool. In: *Proceedings of the 12th Asian Congress of Fluid Mechanics*. Daejeon, Korea.
- Xie, P., Arkin, P.A., 1996. Analyses of global monthly precipitation using gauge observations, satellite estimates, and numerical model predictions. *J. Climate* 9, 840–858.
- Xie, P., Arkin, P.A., 1997. Global precipitation: a 17-year monthly analysis based on gauge observations, satellite estimates and numerical model outputs. *BAMS* 78, 2539–2558.
- Yadav, R.K., Rupa Kumar, K., Rajeevan, M., 2009. Increasing influence of ENSO and decreasing influence of AO/NAO in the recent decades over northwest India winter precipitation. *J. Geophys. Res.* 114, D12112.
- Yadav, R.K., Yoo, J.H., Kucharski, F., Abid, M.A., 2010. Why is ENSO influencing northwest India winter precipitation in recent decades? *J. Climate* 23, 1979–1993.
- Yatagai, A.O., Arakawa, K., Kamiguchi, H., Kawamoto, M., Nodzu, I., Hamada, A., 2009. A 44-year daily gridded precipitation dataset for Asia based on a dense network of rain gauges. *SOLA* 5, 137–140. <http://dx.doi.org/10.2151/sola.2009-035>.